

1N-38

35011

15P

An NDE Approach for Characterizing Quality Problems in Polymer Matrix Composites

Don J. Roth, George Y. Baaklini, and James K. Sutter
National Aeronautics and Space Administration
Lewis Research Center
Cleveland, Ohio

James R. Bodis
Cleveland State University
Cleveland, Ohio

Todd A. Leonhardt
NYMA Inc.
Engineering Services Division
Brook Park, Ohio

Elizabeth A. Crane
John Carroll University
University Heights, Ohio

Prepared for the
40th International Symposium and Exhibition
sponsored by the Society for the Advancement of Materials and Process Engineering
Anaheim, California, May 8-11, 1995



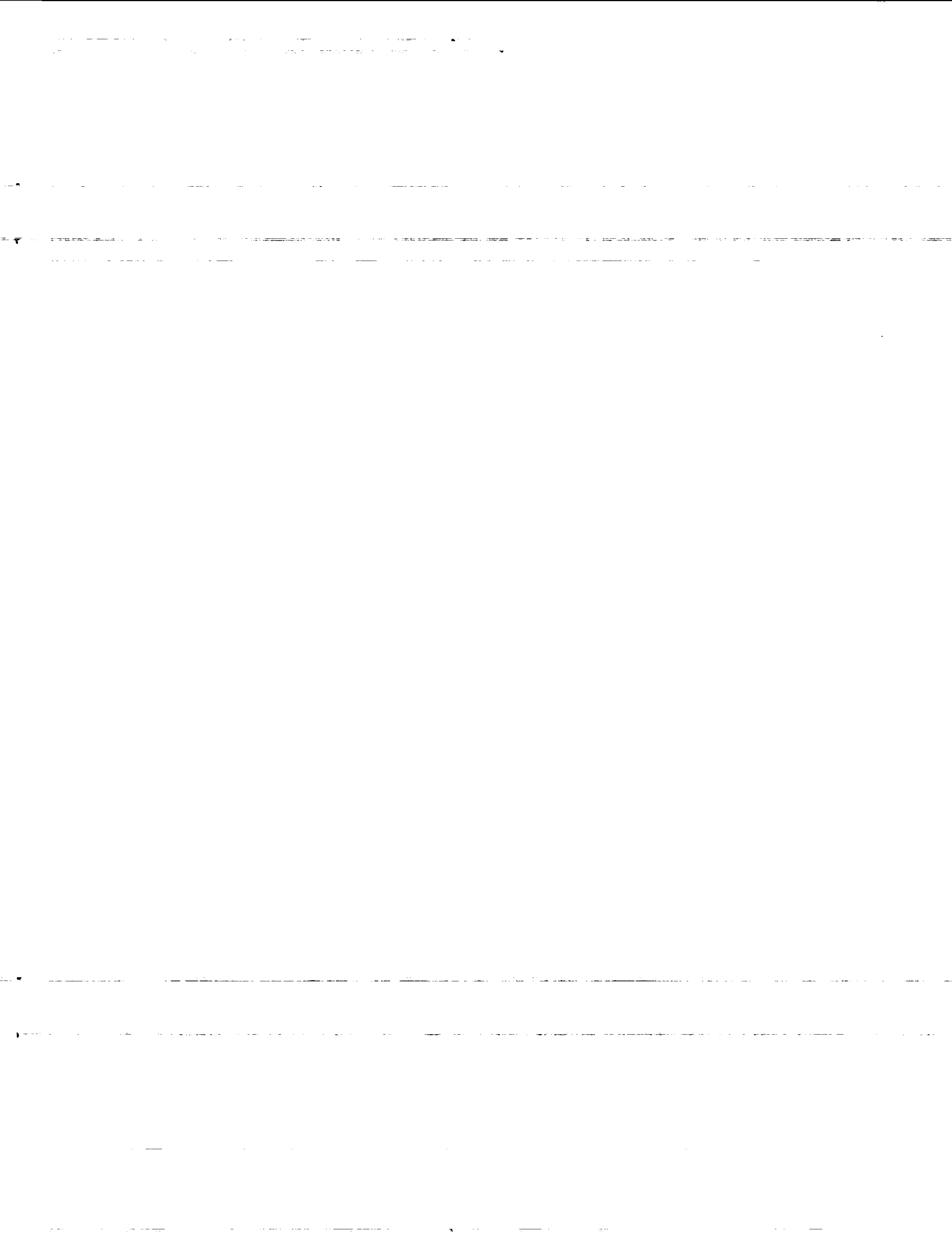
National Aeronautics and
Space Administration

(NASA-TM-106807) AN NDE APPROACH
FOR CHARACTERIZING QUALITY PROBLEMS
IN POLYMER MATRIX COMPOSITES
(NASA. Lewis Research Center) 15 p

N95-18583

Unclass

G3/38 0035011



AN NDE APPROACH FOR CHARACTERIZING QUALITY PROBLEMS IN POLYMER MATRIX COMPOSITES

Don J. Roth, George Y. Baaklini, James K. Sutter
National Aeronautics and Space Administration
Lewis Research Center
Cleveland, Ohio 44135

James R. Bodis
Cleveland State University
Cleveland, Ohio 44115

Todd A. Leonhardt
NYMA, Inc.
Engineering Services Division
Brook Park, Ohio 44142

Elizabeth A. Crane
John Carroll University
University Heights, Ohio 44118

ABSTRACT

Polymer matrix composite (PMC) materials are periodically identified appearing optically uniform but containing a higher than normal level of global nonuniformity as indicated from preliminary ultrasonic scanning. One such panel was thoroughly examined by nondestructive (NDE) and destructive methods to quantitatively characterize the nonuniformity. The NDE analysis of the panel was complicated by the fact that the panel was not uniformly thick. Mapping of ultrasonic velocity across a region of the panel in conjunction with an error analysis was necessary to 1) properly characterize the porosity gradient that was discovered during destructive analyses and 2) account for the thickness variation effects. Based on this study, a plan for future NDE characterization of PMCs is presented to the PMC community.

KEY WORDS: Nondestructive Testing, Polymer Matrix Composites, Ultrasonics

1. INTRODUCTION

Nonuniformity in polymer matrix composite (PMC) parts must be accurately characterized with regards to microstructural nature and severity and the resulting effect on physical properties. This is required so that 1) a decision on whether such a part is unacceptable for further processing, testing or application can be made, 2) if in fact the part is unacceptable, the processing step(s) responsible for the nonuniformity can be pinpointed and modified, 3) nondestructive evaluation (NDE) procedures can be implemented allowing quality decisions to be based primarily on nondestructive characterization. The objective of this work was to use nondestructive and destructive methods to characterize nonuniformity in a PMC panel containing a 150 μm thickness variation. This thickness variation, not an uncommon result of polymer processing methods, complicates NDE analysis. A novel NDE approach is required to determine whether a microstructural gradient exists in addition to thickness variation.

2. EXPERIMENTAL

2.1 Material The panel in this study was a 12-ply unidirectional laminate composed of 40 vol % N-CYCAP resin (1) and 60 vol % T40-R graphite fiber (unsized) in 12000 fibers/tow (Figure 1). It was processed using simulated autoclave vacuum bag methods with final processing conditions of 200 psi (press assist) at 371 °C (2). The panel dimensions were 20.5 cm by 7.5 cm by ~ 0.2 cm thick. The thickness of the panel was measured at 20 locations across the panel. For these locations, thickness varied from 1.946 mm to 2.103 mm, a variation of 0.157 mm. The following trends in thickness were noted: 1) the top and bottom edge areas were generally 0.050 to 0.150 mm less thick than the interior regions and 2) thickness increased from right to left along several interior lines in the panel as shown in Figure 2. The variation in the thickness complicated conventional ultrasonic and radiographic analyses since thickness increases attenuation in both modalities.

2.2 Conventional NDE Through-transmission immersion ultrasonic c-scanning, routinely used to screen for significant within-panel nonuniformity of cured PMCs, was performed on the panel with a 5 Mhz longitudinal wave focused transducer. With the discovery of nonuniformity, high resolution immersion pulse-echo c-scan characterization was performed with a 10 Mhz longitudinal wave focused transducer. The high resolution inspection consisted of a 960 (length-direction) by 416 (width-direction) grid of measurements with each measurement separated from the next by 0.22 mm. The transducer was placed closer to the sample front surface than the focal length (2.54 cm) to obtain measurable back wall reflection.

The panel was then inspected using through-transmission film radiography with a source-to-panel distance of 30" and exposure conditions of 60 kV, 25 mA, and 2 min. Radiographic print images show x-ray attenuation in terms of gray scale with lighter gray scale corresponding to lower x-ray attenuation. Based on previous studies of x-ray detection of density variations in ceramics (3), a uniform x-ray print indicates density variations below approximately 2% *if thickness variations are insignificant*.

2.3 Unconventional NDE: Ultrasonic Contact Scanning An ultrasonic contact scan procedure (Figure 3) (4) was performed over the panel region where significant nonuniformity was indicated from the ultrasonic c-scans. This procedure was performed for the purposes of mapping precise ultrasonic velocity and attenuation coefficient variation. These maps provide more quantitative

information regarding material gradients than conventional ultrasonics since actual ultrasonic wave parameters in the material are being measured. Velocity and attenuation coefficient mapping have been shown to be very sensitive to microstructural gradients (4-6). The contact scan consisted of a 41 (length-direction) by 21 (width-direction) grid of measurements with each measurement separated from the next by 2 mm. The transducer used was unfocused 5 MHz longitudinal wave having a silica buffer rod.

The velocity and attenuation coefficient maps were calculated using a fixed value for thickness. For the velocity calculation

$$V = \frac{2T}{\tau} \quad (1)$$

where V is velocity, T is thickness and τ is time delay between successive back surface ultrasonic echoes. The cross-correlation method, found to minimize the error introduced by noisy waveforms (7), was used to obtain the time delay. The time delay for which the correlation function was a minimum was obtained in the cross-correlation algorithm to account for a phase inversion of echo B2 relative to B1 (7). Actual thickness greater than that used in the velocity calculation results in greater time delay between back surface echoes and thus lower apparent velocity. (Note that the intrinsic velocity in the material is not a function of thickness). To determine the velocity variation expected due to the time delay measurement error and thickness variation over the region scanned, the following equation was used:

$$\% \text{ VARIATION}_{\text{velocity}} = 100 \left[\left(\frac{\Delta T}{T} \right)^2 + \left(\frac{\Delta \tau}{\tau} \right)^2 \right]^{0.5} \quad (2)$$

where ΔT is variation in thickness and $\Delta \tau$ is time delay error.

2.4 Destructive Characterization: Optical Image Analysis The panel was cut at various locations to form sections approximately 0.5 - 1 cm in length. Four cross-sections were mounted and optically viewed with fibers running left-to-right in relation to the viewer, and four cross-sections were mounted and optically viewed with fiber circular cross-sections facing the viewer. After optically viewing each of the sections at 100x, the sections were examined two more times after removing 1 mm of material each time. For the last cut of each section, approximately 10 measurements of pore fraction covering 80 - 90% of the section were made using optical image analysis. The analysis was performed with the Quantimet 500 image analysis system at 125x using a gray level thresholding feature. The threshold was held constant for all sections so that relative error between pore fraction measurements in each frame was low.

3. RESULTS AND DISCUSSION

3.1 Conventional NDE Figure 4 shows the image generated by mapping the peak height of the wave transmitted through the PMC panel in the initial c-scan screening procedure. Figure 5 shows the image generated by mapping the peak height of the echo reflected from the panel back wall during the high resolution pulse-echo c-scan. In both images, white, black and gray color represent low, high and intermediate ultrasonic attenuation, respectively. As shown in Figures 4 and 5, The PMC panel was observed from the immersion ultrasonic procedures to

exhibit a “wavefront” nonuniformity. The wavefront pattern indicates a fairly continuous gradient from right to left of lower to higher attenuation, respectively. Given that the surface condition was uniform across the panel, it can be concluded from the image and the waveform amplitudes that the left end of the panel contained some attenuating microstructural anomaly or thickness increase as compared to the right end.

The radiographic print shown in Figure 6 indicates a uniform gray scale indicating little or no nonuniformity. This was puzzling considering the ultrasonic immersion results shown in Figures 4 and 5; the explanation will be provided in later discussion.

3.2 Unconventional NDE: Ultrasonic Contact Scanning Figure 7 shows the velocity image derived from the ultrasonic contact scan performed over the transition region of the wavefront nonuniformity. The image is presented with a line drawn across it which shows the average velocity trend across the sample region and indicates decreasing velocity from right to left. Higher-to-lower velocity variation such as this is usually attributable to increasing thickness or a microstructural component gradient (4,5). The total velocity variation across the scanned region was 10.7% as calculated from:

$$\% \text{VARIATION}_{\text{velocity}} = 100 \frac{\text{Velocity}_{\text{MAX}} - \text{Velocity}_{\text{MIN}}}{\text{Velocity}_{\text{MAX}}} \quad (3)$$

The time delay error, ΔT only contributed 0.1% to the percent velocity variation. Using $\pm 0.050 - \pm 0.100$ mm as a range for thickness variation ΔT over the scanned region, thickness variation contributed 2.5–5% to the percent velocity variation. From Equation 2, the latter results leaves 5 – 7.5% variation above and beyond that due to time delay error and thickness variation. Thus, it was concluded that a microstructural gradient must have been responsible for the remaining velocity variation. Note that it was possible to quantify the variation associated with the microstructural variation only by using the velocity mapping method and error analysis in conjunction with thickness measurements. A new imaging method presently being commercially developed in a cooperative effort between NASA and Sonix, Inc. uses a single transducer scan procedure to eliminate thickness effects. Thus, the resulting image will show only true microstructural variation.

The attenuation coefficient map of the same region is presented with a line drawn across it in Figure 8. The line shows the average attenuation coefficient trend across the sample region and indicates increasing attenuation coefficient from right to left which is consistent with increasing sample thickness and / or greater scattering (4). A much more complicated error analysis than that used for velocity variation is necessary to separate effects on attenuation coefficient variation due to thickness and microstructural effects (4). A recent study showed a novel two transducer method for obtaining attenuation images independent of thickness (8).

3.3 Destructive Characterization: Optical Image Analysis In viewing the cross-sections cut from the panel, it was apparent that a pore fraction gradient existed across the panel from right-to-left. The average percent porosities obtained from image analysis are given next to the section labels in Figure 9. The porosity was elongated in the direction of the fiber; hence the consistent difference in pore fractions for the two different viewing orientations. In the direction parallel to the fibers, average percent porosity increased from $\sim 0\%$ at the right end to $0.7 \pm 0.3 \%$ in the center

to $2.7 \pm 0.8\%$ at the left end of the panel. The processing step where the pores originated needs to be determined. Pores in PMCs can result from a number of sources including trapped air in fiber bundles, condensation reaction procedures, residual solvent from prepregging, low molecular weight polymer chains that degrade and volatilize during processing, and decomposition of larger polymer chains during high temperature processing or post processing (postcure). Two possible causes of pore fraction *variations* in PMCs include a misaligned platen causing uneven pressure during pressing, or one end of the panel "stiffening" so resin flow is impeded during pressing. The pore fraction variations seen in the panel can lead to significant property variation. For example, it has been observed that interlaminar shear strength was reduced 15% when percent porosity increased from 0 to 1% in PMC material (9).

3.4 Correlation of NDE results with Microstructure Based on the error analysis results for velocity mapping, the pore fraction gradient observed in the panel was responsible for the percent velocity variation above and beyond that due to thickness variation seen in the velocity map. Although the pore fraction *over the region of the velocity map* increased only $\sim 1\%$ from right-to-left as measured from the optical image analysis, this increase accounted for a 5–7% decrease in velocity (excluding that due to thickness variation and time delay error). The decrease in velocity with increasing pore fraction is consistent with previous investigations for other materials, although the 5–7% decrease in velocity for a 1% increase in porosity is larger than that seen previously for metals and ceramics (6).

With regards to velocity and attenuation mapping for both contact and immersion scanning, thickness variation can mask or complement microstructural variation depending on whether it spatially opposes or complements the microstructural variation. In this investigation, thickness increased (causing apparent velocity decrease and attenuation increase) in the same direction as pore fraction increased (causing real velocity decrease and attenuation increase) so that the effects complemented each other with regards to velocity and attenuation measure. It has been previously exhibited that attenuation increases with increasing thickness and increasing pore fraction in graphite - polymer composites (10).

It is also possible to explain the relative uniformity of the radiograph shown in Figure 6. Again, thickness variation can mask or exaggerate microstructural variation on x-ray attenuation images depending on the spatial relation of the variations. Thickness increase causes an increase in x-ray attenuation while pore fraction increase causes a decrease in x-ray attenuation. Since thickness and pore fraction generally increased from right-to-left across the panel, the effect due to the thickness increase masked the effect due to the pore fraction increase in the x-ray attenuation image. Thus, the x-ray print appeared relatively uniform.

4. FURTHER DISCUSSION

4.1 Post-scan Interactive Data Display System A post-scan interactive data display system (PSIDD) has been developed at NASA Lewis Research Center for viewing raw waveform (digitized) data and resulting properties (Fourier spectra, phase velocity, attenuation coefficient, reflection coefficient versus frequency) at any scan location on any of the ultrasonic images formed from ultrasonic contact scans (11). Based on a waveform distortion and property analysis software routine, scan locations can be highlighted on video display where raw waveform data are deemed distorted and / or property values are considered questionable. This type of analysis is extremely sensitive for detecting waveform distortions that indicate microstructural

inhomogeneity even when the ultrasonic image does not indicate prominent inhomogeneity at that scan point. The use of these PMC materials in high-performance applications may require such analysis to pinpoint subtle variations in microstructure. The criterion used to flag distorted waveforms was that the Fourier magnitude of either of the back-surface echoes had a significant double-peaked characteristic. Figure 10 shows the ultrasonic velocity image of Figure 7 with several scan locations highlighted by short vertical lines. These locations are more prevalent at the porous (left), lower velocity end of the scanned region but do not show striking gray scale variations in relation to neighboring scan points in the image. However, time-domain back surface waveforms ($B2(T)$) at these scan locations exhibited above average noise which resulted in a double-peak (destructive interference) characteristic for the corresponding Fourier magnitude spectra ($B2(F)$) as compared to those for surrounding scan locations. It is likely that specific elongated pores or pore clusters caused ultrasonic scatter and the resulting distorted waveforms and destructive interference characteristic of the magnitude spectra. Another example of PSIDD analysis is shown in Figure 11 where a PMC panel exhibiting less than 1% pore fraction variation across the panel still has many locations near the top and bottom edges showing highly-distorted waveforms. In Figure 11, waveform distortion correlated with higher-than-average attenuation coefficient and lower-than-average velocity positions for most but not all positions.

4.2 Recommendations A hierarchal approach to quality control of PMCs is suggested in the flowchart of Figure 12 based on results of this study. Each step of fabrication for PMCs that potentially can result in "serious" microstructural nonuniformity, and the resulting different types of microstructural nonuniformity, need to be identified. Then, a study combining NDE and destructive characterization to correlate NDE results with microstructure should be performed as was done in this study. Screening level NDE can include c-scan, radiography, and thickness measurement. If needed, more detailed NDE can include precision ultrasonic velocity mapping and waveform distortion analysis. Most desired would be to perform NDE at all potentially problematic steps of fabrication, preferably in-process. For PMC processing, it is likely that such studies will be most practical at the cure and post-cure steps. These studies will allow the choice of necessary NDE methods, and calibration and standardization of the NDE methods, so that future characterization of nonuniformity in PMC's primarily can be performed nondestructively. Then, a problem can be identified and corrected before continuing additional processing that will only result in a rejected part. NDE characterization should nearly always include complementary NDE methods to obtain accurate and corroborative results as evidenced in this study where radiographic results did not reveal microstructural nonuniformity.

5. CONCLUSIONS

The origin of the "wavefront" nonuniformity in a PMC panel was determined via nondestructive and destructive methods to be a combination of thickness and pore fraction variation. A complementary array of NDE methods in conjunction with velocity error analysis was required to properly characterize the nonuniformity. A hierarchal approach involving NDE for process control of PMCs is suggested.

6. REFERENCES

1. J.K. Sutter, et al.: Long Term Isothermal Aging and Thermal Analysis of N-CYCAP Polyimides. NASA TM-104341, 1991.

2. J.F. Waters, J.F., et.al.: Addition Curing Thermosets Endcapped with 4-Amino[2.2]paracyclophane. J.Polymer Science Part A - Polymer Chemistry, Vol. 29, 1991, pp. 1917-1924.
3. G.Y. Baaklini, et.al.: Probability of Detection of Internal Voids in Structural Ceramics Using Microfocus Radiography. J. Mater. Res., Vol. 1, No. 3, 1986. pp. 457- 467.
4. D.J. Roth, et. al.: Quantitative Mapping of Pore Fraction Variations in Silicon Nitride Using an Ultrasonic Contact Scan Technique. NASA TP-3377. 1993.
5. Roth, D.J., et. al.: Spatial Variations in A.C. Susceptibility and Microstructure for the $\text{YBa}_2\text{Cu}_3\text{O}_{7-x}$ Superconductor and Their Correlation with Room-temperature Ultrasonic Measurements. J. Mater. Res., Vol. 6, No. 10, 1991.
6. D.J. Roth, et. al.: Review and Statistical Analysis of the Ultrasonic Velocity Method for Estimating the Porosity Fraction in Polycrystalline Materials. NASA TM-102501. 1990. Also, Materials Evaluation, Vol. 49, No. 7, 1991. pp. 883-888.
7. D.R. Hull, et. al.: Measurement of Ultrasonic Velocity Using Phase-Slope and Cross-Correlation Methods. Materials Evaluation, Vol. 43, No. 11, 1985, pp. 1455-1460.
8. M. Bashyam: Thickness Compensation and Dynamic Range Improvement For Ultrasonic Imaging of Composite Materials. Review of Progress in Quantitative Nondestructive Evaluation: Proceedings of the 17th Annual Review, La Jolla, CA, July 15-20, 1990. Vol. 10A. New York, Plenum Press, 1991, pp. 1035-1042.
9. K. Bowles, et al.: Void Effects on the Interlaminar Shear Strength of Unidirectional Graphite-Fiber-Reinforced Composites. J. Comp. Mat., Vol. 26, No. 10, 1992, pp. 1487-1509.
10. P. Shen, et al.: Ultrasonic Attenuation Measurement and Its Application in Porosity Evaluation of Composite Materials. ASNT 1992 Spring Conference, Orlando, Florida, Mar. 30-Apr. 3, 1992.
11. D.J. Roth and S.A. Szatmary: PSIDD: A Post-Scan Interactive Data Display System for Ultrasonic Scans. NASA TM-4545. 1993.

- 12-ply Unidirectional
- 40 vol % N-CYCAP resin matrix
- 60 vol % T40-R graphite fiber (12 K TOW) (unsized)
- Simulated autoclave vacuum bag methods
- Final conditions: 200 psi at 371 °C

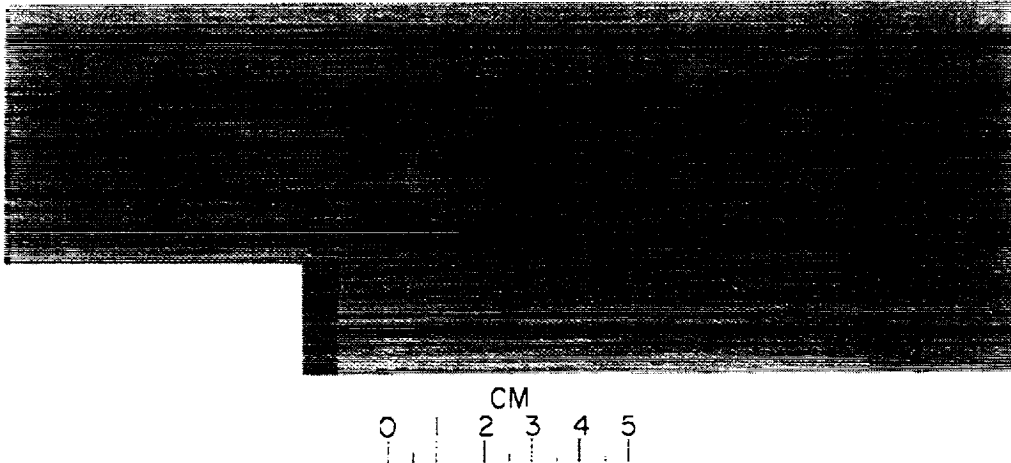


Figure 1.—PMC material description.

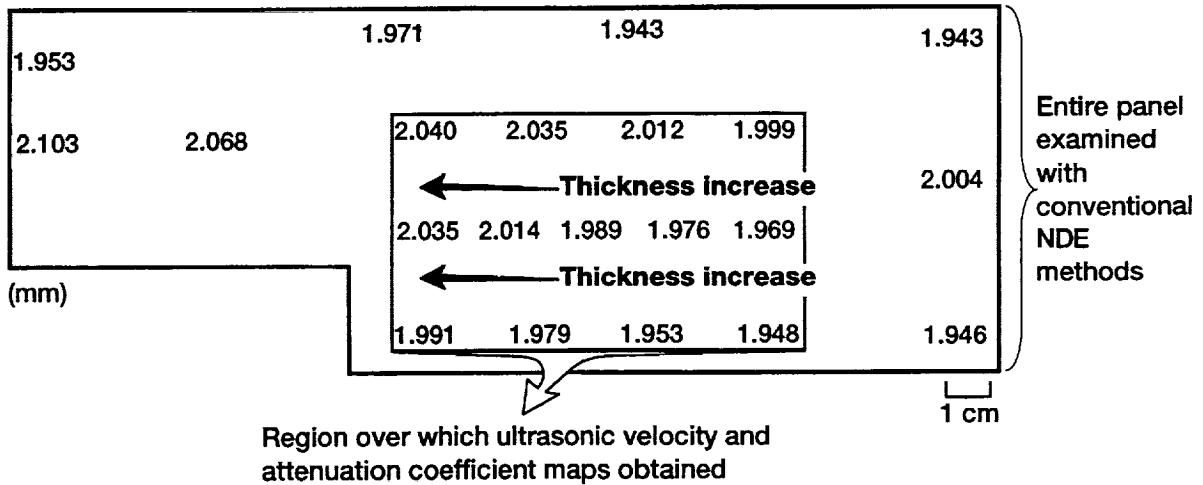


Figure 2.—Panel thickness variation (numbers indicate thickness in millimeters). Thickness is lowest at top and bottom edge areas; interior thickness increases from right to left.

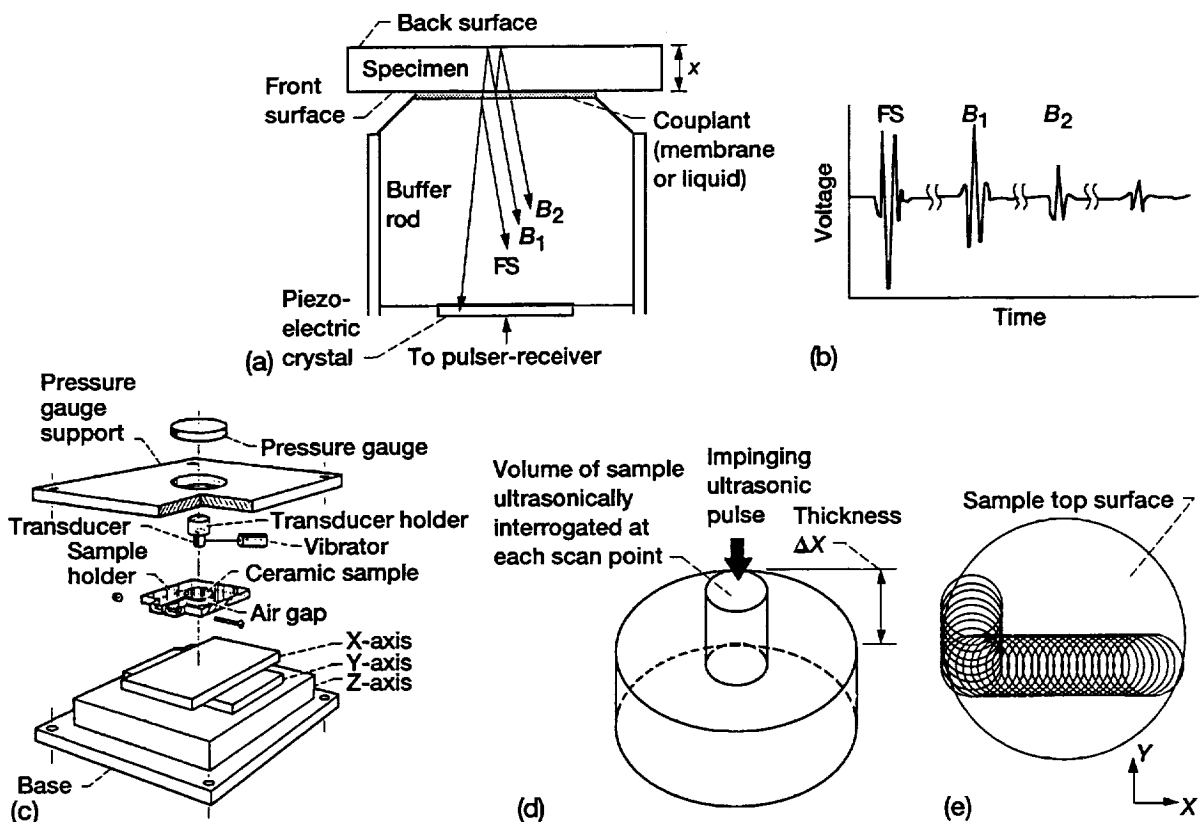


Figure 3.—Ultrasonic contact scan measurement method (FS = front-surface reflection; B_1 = first back-surface reflection; B_2 = second back-surface reflection). (a) Diagram of buffer rod-couplant-sample pulse-echo contact configuration. (b) Resulting waveforms for pulse-echo contact technique. (c) Scanner hardware. (d) Schematic (three-dimensional view) showing volume of sample ultrasonically interrogated at each scan point for velocity and attenuation coefficient measurements. (e) Schematic (top view) of ultrasonic contact scan procedure showing examples of successive transducer positions along X- and Y-dimensions of sample.

- Initial quality screening
- Note "wavefront-like" nonuniformity
- White is lowest attenuation
- Grey is intermediate attenuation
- Black is highest attenuation

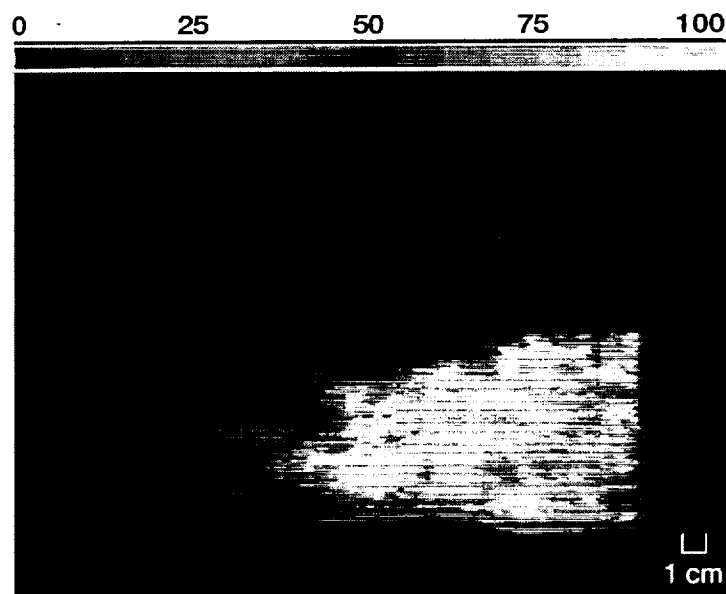


Figure 4.—Ultrasonic through-transmission C-SCAN (5 MHz).

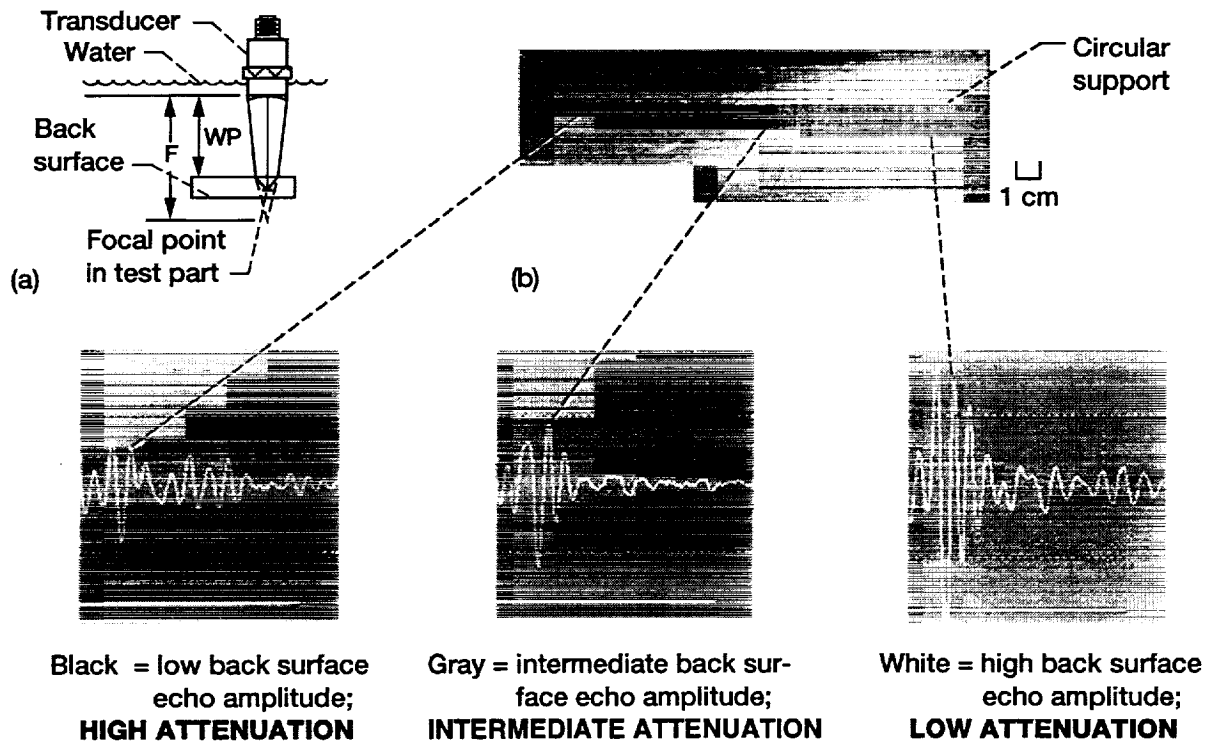


Figure 5.—High-resolution back echo ultrasonic C-SCAN. Back surface echo gate for volumetric imaging. F \equiv nominal focal length. WP \equiv water path length. (a) Schematic of set-up for back surface echo gating. (b) Back surface echo image and back surface echoes at three locations.



Figure 6.—Film radiography. Source-to-panel distance = 30 in., 60 kV, 25 mA, 2 min. Panel appears uniform. Indicates density variations below ~ 2% if thickness variations insignificant.

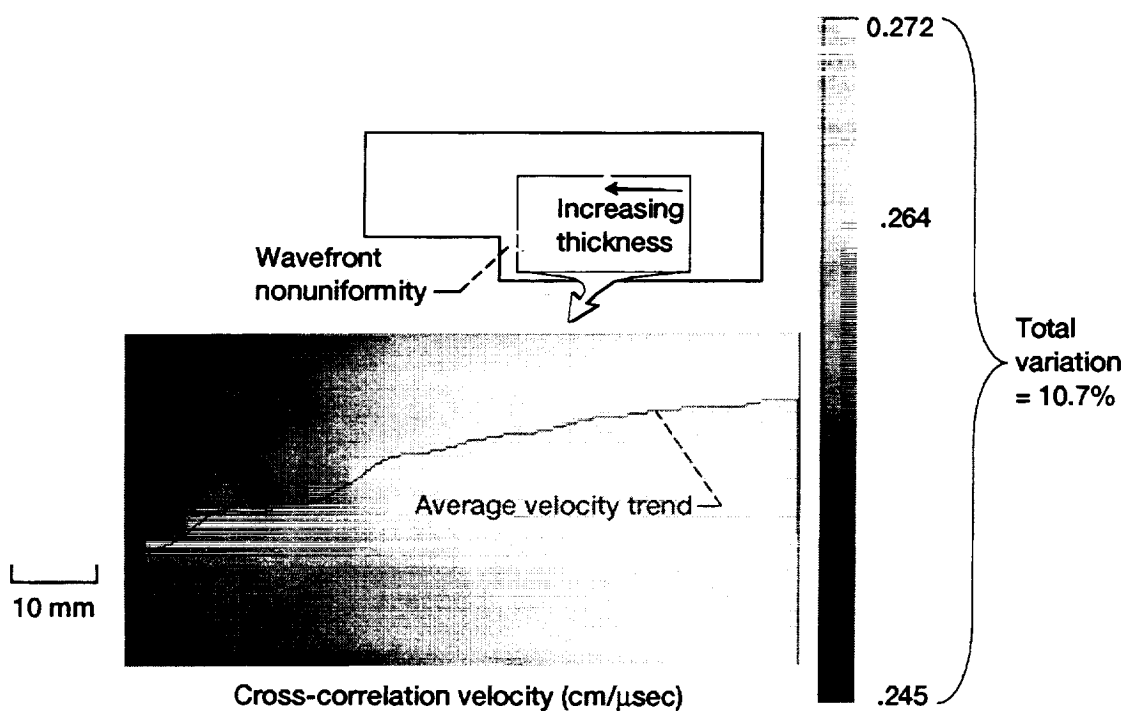


Figure 7.—Ultrasonic velocity mapping. Left-to-right velocity variation indicates thickness and/or microstructural gradient.

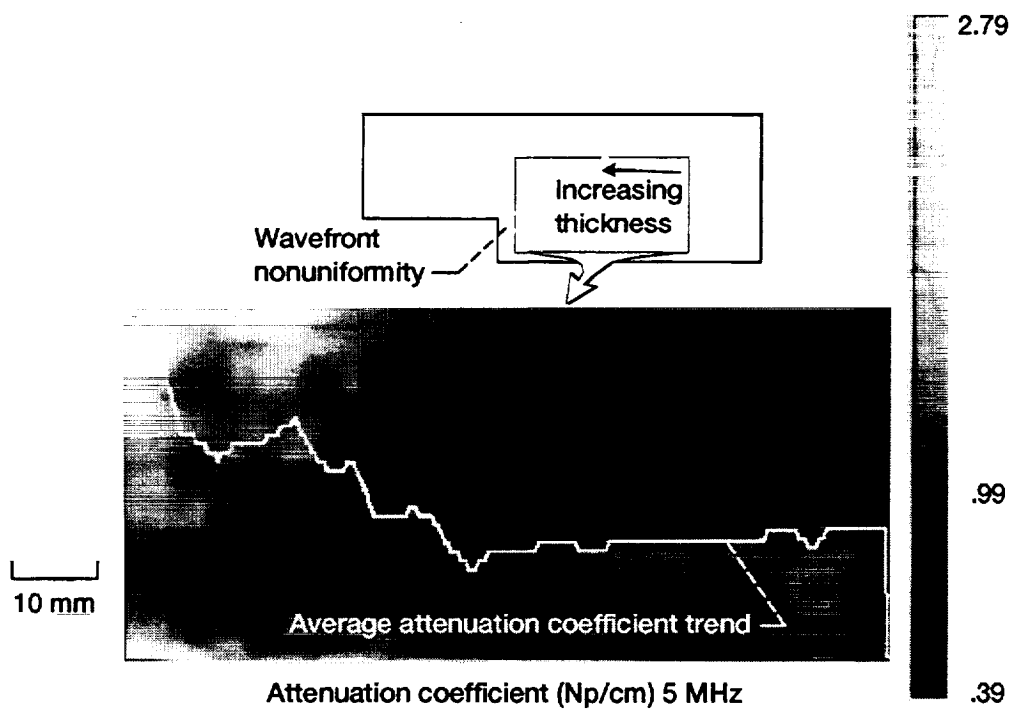


Figure 8.—Ultrasonic attenuation coefficient mapping. Left-to-right attenuation coefficient variation indicates thickness and/or microstructural gradient.

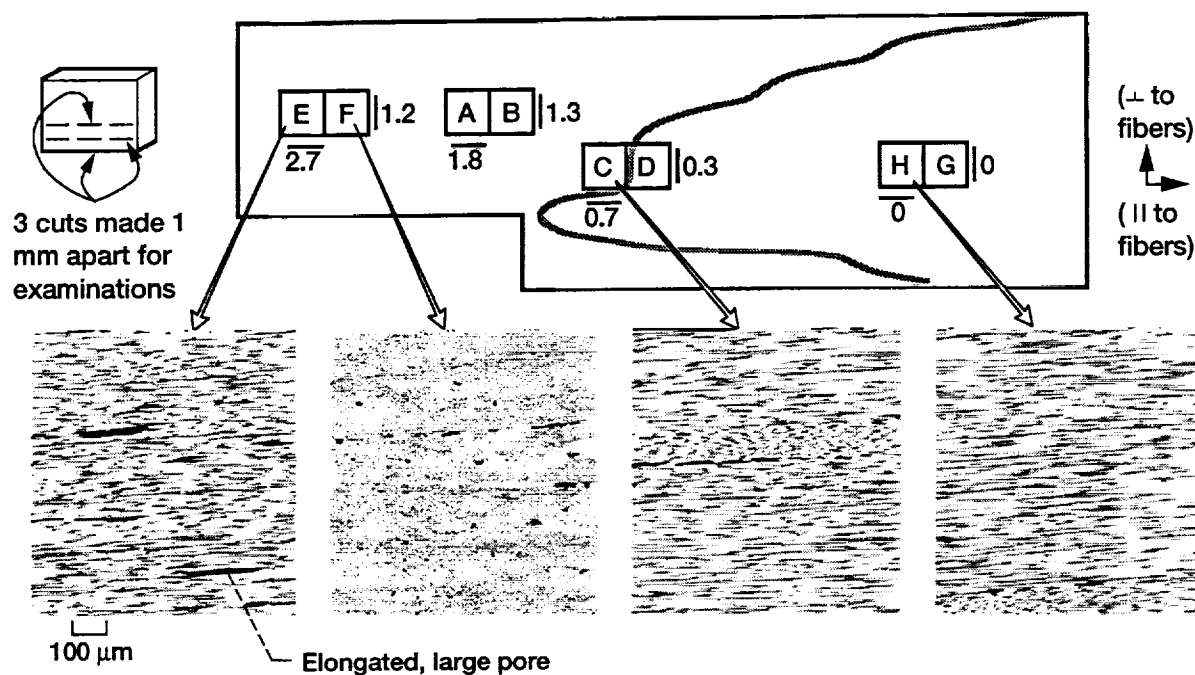


Figure 9.—Destructive sectioning and optical image analysis. Numbers show % porosities. Note porosity gradient (high at left and low at right).

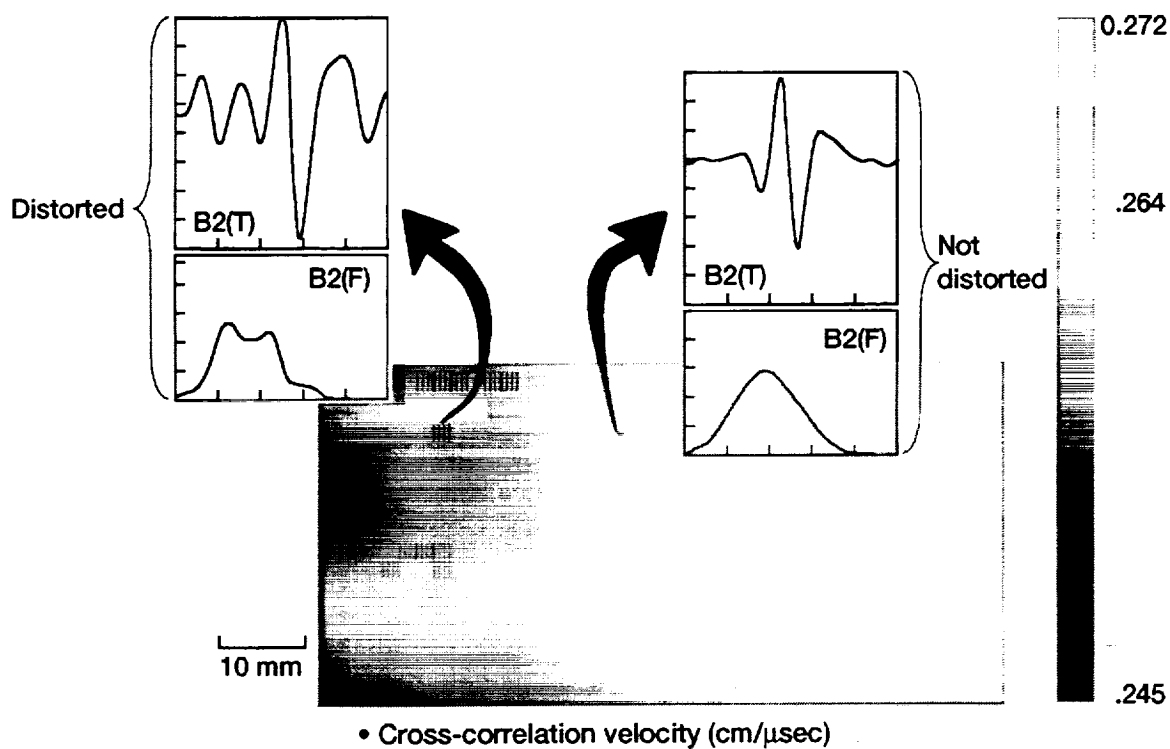


Figure 10.—Post-scan interactive data display for waveform analysis. Scan locations highlighted by small vertical lines where waveforms distorted.

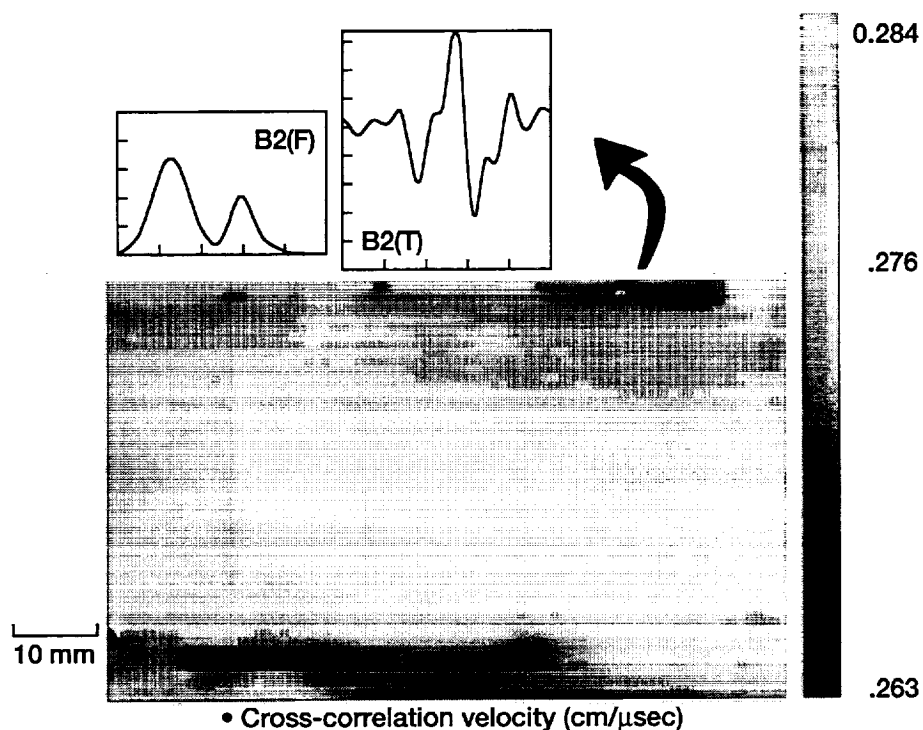


Figure 11.—Post-scan interactive data display for waveform analysis. Scan locations highlighted by small vertical lines where waveforms distorted.

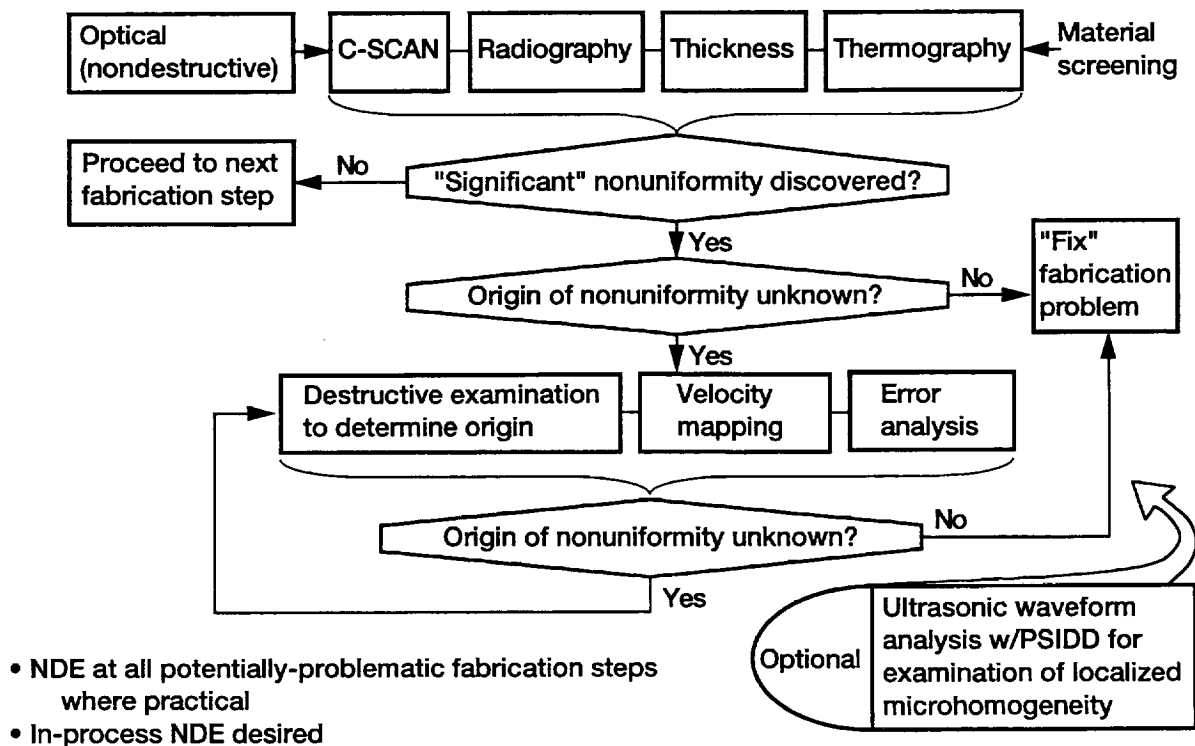


Figure 12.—NDE hierarchy for PMC examination and process control.

REPORT DOCUMENTATION PAGE			Form Approved OMB No. 0704-0188	
Public reporting burden for this collection of information is estimated to average 1 hour per response, including the time for reviewing instructions, searching existing data sources, gathering and maintaining the data needed, and completing and reviewing the collection of information. Send comments regarding this burden estimate or any other aspect of this collection of information, including suggestions for reducing this burden, to Washington Headquarters Services, Directorate for Information Operations and Reports, 1215 Jefferson Davis Highway, Suite 1204, Arlington, VA 22202-4302, and to the Office of Management and Budget, Paperwork Reduction Project (0704-0188), Washington, DC 20503.				
1. AGENCY USE ONLY (Leave blank)	2. REPORT DATE December 1994	3. REPORT TYPE AND DATES COVERED Technical Memorandum		
4. TITLE AND SUBTITLE An NDE Approach for Characterizing Quality Problems in Polymer Matrix Composites		5. FUNDING NUMBERS WU-505-63-12		
6. AUTHOR(S) Don J. Roth, George Y. Baaklini, James K. Sutter, James R. Bodis, Todd A. Leonhardt, and Elizabeth A. Crane				
7. PERFORMING ORGANIZATION NAME(S) AND ADDRESS(ES) National Aeronautics and Space Administration Lewis Research Center Cleveland, Ohio 44135-3191		8. PERFORMING ORGANIZATION REPORT NUMBER E-9292		
9. SPONSORING/MONITORING AGENCY NAME(S) AND ADDRESS(ES) National Aeronautics and Space Administration Washington, D.C. 20546-0001		10. SPONSORING/MONITORING AGENCY REPORT NUMBER NASA TM-106807		
11. SUPPLEMENTARY NOTES Prepared for the 40th International SAMPE Symposium and Exhibition sponsored by the Society for the Advancement of Materials and Process Engineering, Anaheim, California, May 8-11, 1995. Responsible person, Don J. Roth, organization code 5250, (216) 433-6017.				
12a. DISTRIBUTION/AVAILABILITY STATEMENT Unclassified - Unlimited Subject Category 38 This publication is available from the NASA Center for Aerospace Information, (301) 621-0390.		12b. DISTRIBUTION CODE		
13. ABSTRACT (Maximum 200 words) Polymer matrix composite (PMC) materials are periodically identified appearing optically uniform but containing a higher than normal level of global nonuniformity as indicated from preliminary ultrasonic scanning. One such panel was thoroughly examined by nondestructive (NDE) and destructive methods to quantitatively characterize the nonuniformity. The NDE analysis of the panel was complicated by the fact that the panel was not uniformly thick. Mapping of ultrasonic velocity across a region of the panel in conjunction with an error analysis was necessary to 1) properly characterize the porosity gradient that was discovered during destructive analyses and 2) account for the thickness variation effects. Based on this study, a plan for future NDE characterization of PMCs is presented to the PMC community.				
14. SUBJECT TERMS Nondestructive testing; Polymer matrix composites; Ultrasonics; Porosity; Ultrasonic velocity		15. NUMBER OF PAGES 15		
		16. PRICE CODE A03		
17. SECURITY CLASSIFICATION OF REPORT Unclassified	18. SECURITY CLASSIFICATION OF THIS PAGE Unclassified	19. SECURITY CLASSIFICATION OF ABSTRACT Unclassified	20. LIMITATION OF ABSTRACT	